J. Plasma Fusion Res. SERIES, Vol. 4 (2001) 403–407

Effects of Radial Electric Field on Neoclassical Transport in Helical Torus

SANUKI Heiji*, TODOROKI Jiro and NAKAGAWA Tadashi[A),**]
National Institute for Fusion Science, Toki-shi, Gifu, 509-5292, Japan
[A)]Department of Energy Engineering and Science, Nagoya University, Nagoya 464-01, Japan

(Received: 5 December 2000 / Accepted: 27 August 2001)

Abstract

The poloidal rotation of particles may be modified in the presence of radial electric field, leading the improvement of particle confinement. For a specific electric field, however, there exists a degradation of particle confinement cased by so-called helical and/or toroidal resonance. The structure of the boundary layers and transport coefficients in cases with and without resonance are studied in detail by using a numerical code for solving the bounce-averaged Fokker-Planck equation.

Keywords:

radial electric field, confinement improvement, resonance, neoclassical transport, helical torus

1. Introduction

A powerful tool for analyzing the particle orbit topologies and related structure of trapped and passing particles in helical torus has been discussed by solving the drift kinetic equation for plasmas with 3-D toroidal geometry. Numerical codes based on this type of tool, such as the DKES code [1] and the PFSTL code [2] have been developed to study the neoclassical transport. In the previous papers [3,4], the analytic representation for the longitudinal adiabatic invariant for the general magnetic configuration instead of a simple model magnetic field, is presented in the convenient form for the numerical calculations for realistic magnetic configurations. A powerful method based on such expression was applied to the study of the transport in the wide range of parameter space specifying the magnetic field geometry.

The $E\times B$ poloidal rotation may suppress the loss of helical trapped particles and it consequently leads the improvement of particle confinement. For a specific value of electric field, however, there is a possible degradation of particle confinement caused by so-called helical and/or toroidal resonance [5]. The analytical and numerical results have not been completely understood, particularly when a boundary layer associated with a radial electric field is present. In the present study, the effect of radial electric field on neoclassical transport is analyzed in detail.

A model magnetic field is frequently employed in most neoclassical transport theories for simplicity, but the magnetic field are now calculated by using the MAGN code [3,6] for fixed coil currents. Then, the transport coefficients are evaluated for a realistic magnetic field, such as one based on the large helical device (LHD) parameters. Comparison between these results and the results based on the DKES code [7,8] has also been made.

2. Bounce-Averaged-Fokker-Planck Equation

In the helical torus of our interest, the system as a large number of field periods N in the toroidal direction (ϕ) and the rotational transport per period is small.

*Corresponding author's e-mail: sanuki@nifs.ac.jp
**Present address: Matsushita Electric Industrial Co., Ltd., Takatsuki, Osaka, Japan

Under this assumption, the particle motion can be separated into the fast periodic motion in ϕ-direction and the slower motion perpendicular to this direction. After averaging with respect to the fast periodic motion, the slow motion can be described in terms of the longitudinal adiabatic invariant discussed in [3]. In that situation, the main part of the particle distribution function is independent of the toroidal angle, i.e., $f(E, \mu, \sigma, \psi, \vartheta)$, $\sigma = \pm 1$ being the sign of the parallel velocity, and is described by the following bounce-averaged Fokker-Planck equation [4]

$$\frac{1}{e}\frac{\partial J_{//}}{\partial \vartheta}\frac{\partial f}{\partial \psi} - \frac{1}{e}\frac{\partial J_{//}}{\partial \psi}\frac{\partial f}{\partial \vartheta} + \sigma e V_\phi = \bar{C}(f,f), \quad (1)$$

$$J_{//} = -\frac{2\pi e}{N} + \oint \frac{m v_{//} B_\phi}{B} d\phi, \bar{C} = \oint \frac{B}{v_{//} B_\phi} d\phi, \quad (2)$$

with V_ϕ being the loop Voltage, E the energy, μ the magnetic moment, ψ the magnetic surface, ϑ the poloidal angle, and $\bar{C}$ is the bounce-averaged collision term. The rotational transform is related to ψ_p in Eq. (2). If we define the distribution function as $f = f_0(K,\psi)\{1 + h(K,\lambda,\vartheta,\psi)\}$ where $\lambda = \mu B_0/K$, $K = E - e\Phi_E(\psi)$, f_0 is Maxwellian, and also introduce the even part h^+ and the odd part h^- of the distribution function h with respect to the sign of the parallel velocity $v_{//}$, and define the functions

$$h^{\pm c}(\vartheta) = \frac{h^\pm(\vartheta) + h^\pm(-\vartheta)}{2}, \; h^{\pm s}(\vartheta) = \frac{h^\pm(\vartheta) + h^\pm(-\vartheta)}{2} \quad (3)$$

the linearized Fokker-Planck equation reduces to

$$\begin{aligned} &Ch^{+c} + Hh^{-s} + Dh^{+s} = 0, \quad Ch^{-c} + Hh^{+s} + Dh^{-s} = S^{-c}, \\ &Ch^{+s} + Hh^{-c} + Dh^{+c} = S^{+s}, \quad Ch^{-s} + Hh^{+c} + Dh^{-c} = 0, \end{aligned} \quad (4)$$

where

$$S^+ = \frac{1}{e}\frac{\partial J_{//}}{\partial \vartheta}\frac{\partial \ln f_0}{\partial \psi}, S^- = \frac{eV_\phi}{T}, \bar{C} = \nu(v)\frac{\partial}{\partial \lambda} M \frac{\partial}{\partial \lambda},$$

$$M = \oint \frac{m v_{//}}{B^2} d\phi, H = f_0 \iota \frac{\partial}{\partial \vartheta}, D = \omega_E f_0 \left\langle \frac{\partial J_{//}}{\partial K} \right\rangle \frac{\partial}{\partial \vartheta}, \omega_E = \frac{d\Phi_E}{d\psi}.$$

Only the pitch angle scattering term, which is dominant particularly, in the low collisionality region, is retained in the collision operator. Let us discuss the problems associated with the boundary layer and the resonance involved in the solution of Eq. (4). The following two boundary layers appear in the low collisionality limit: (B1) $\lambda_c - \delta_1 < \lambda < \lambda_c$, (B2) $\lambda_* - \delta_2 < \lambda < \lambda_* + \delta_2$ in the case of $\omega_E = 0$, (B3) $\lambda_c - \delta_1 < \lambda < \lambda_c - \delta_3$, and (B4) $\lambda_* - \delta_3 < \lambda < \lambda_* + \delta_3$ in the case of $\omega_E \neq 0$, where, $\delta_1 \equiv \nu/\omega_B$, $\delta_2 \equiv \sqrt{\nu/\omega_B}$, $\delta_3 \equiv \nu/\omega_E$, $\lambda_c(\vartheta) = B_0/B_{\max}$, $\lambda_* = \min \lambda_c$, and $\omega_B = \iota v_{//}/R$. Here, we note that the boundary layer exists only on the passing particle side ($\lambda \leq \lambda_c(\vartheta)$) for $\omega_E = 0$, but it appears in both the passing and trapped regions for $\omega_E \neq 0$. When ω_E becomes large, the so-called helical resonance appears, provided that the resonance condition $\omega_E = \omega_B$ is satisfied.

As for the numerical scheme to solve Eq. (4) effectively, the function in the ϑ direction is expressed in terms of a Fourier expansion, and the meshes with variable distances are concentrated in the region of boundary layers. So, the structure of the solution near boundary layer can be well analyzed. A symmetric band matrix solver is used in the numerical calculations. Then, the computation time is dramatically reduced particularly in the low collisionality region. After solving Eq. (4), the transport coefficients are represented by the following relations:

$$D_{11} \propto (S^{-c}, h^{-c}), D_{13} \propto (S^{+s}, h^{+c}), (a,b) = \int ab d\lambda, \quad (5)$$

where S and h are given by the notations defined below Eq. (4) and the solutions of Eq. (4). We note that D_{11} and D_{13} defined in Eq. (5) correspond to the particle transport coefficient and the bootstrap current, respectively.

3. Numerical Results

In the following discussions, we used a realistic magnetic field, which is calculated, by using the MAGN code for the LHD parameters. It should be noted that the present results reproduce the results based on the DKES code and the analysis is also applicable to some specific resonance cases in which the analysis based on the DKES code is inappropriate.

Typical results for the collisionality dependence of the diffusion coefficient (D_{11}) and the bootstrap current (D_{13}) in the case of the LHD parameters are shown in Fig. 1(a) and Fig. 1(b), respectively, for different values of the normalized radial electric field, $R\omega_E/v$. The parameters used in the calculations are $r/a = 0.5$, $B_0 = 3$ T, $\iota = 0.48$, $\varepsilon_t = 0.074$, and $\varepsilon_h = 0.054$. Figure 1(a) shows that, in the $1/\nu$ collisionality region the diffusion coefficient drastically decreases as the electric field increases. Figure 1(b) indicates that the bootstrap current does not monotonically increase as the collision frequency decreases and that it is very sensitive to the magnitude of the electric field. It turns out from Fig. 1(b) that as the collision frequency decreases, the bootstrap current increases in the banana region and seems to saturate at some collision frequency (at the transition), which depends on the magnitude of the electric field. Then, it decreases with decreasing collision frequency and seems to be independent of both the collisionality and the electric field in the very low collisionality region such as $R\nu/v \leq 10^{-5}$. This behavior of the bootstrap current has been pointed out first by Shaing et al. [9] and similar results were reported in [7]. In the present research, however, the asymptotic behavior of the bootstrap current has been studied in further low collisionality region than it was in [7]. The results show more clearly that the bootstrap current is rather independent of the collisionality and is insensitive to the electric field in such a parameter region. We next consider the influence of the resonance on the transport. The distribution function may be deformed by the resonance between the bouncing and the electric rotation when the resonance condition, $\iota v_{//}/R \cong \omega_E$ is satisfied. The coefficient D_{11} versus $R\nu/v$ are shown in Fig. 2 for several values of $R\omega_E/v$. Here, the case with $R\omega_E/v = 10^{-1}$corresponds to the case of the resonance. Although the diffusion coefficients are reduced due to the electric field as shown in Fig. 1(a), it grows again once the resonance appears. With further increase of the electric field, however, the resonance may vanish for a specific level of the electric field, where $\lambda \cong 0$, and consequently, the sudden changes of the transport coefficients are observed. Typical 2-D constant contours in the $\lambda - \vartheta$ plane for the even (h^+) and add (h^-) parts of the distribution function are plotted in Fig. 3 for three typical values of the normalized electric field parameters. The solid and dotted lines in the contour plot correspond to the positive and negative parts of the distribution function, respectively. As was shown in Fig. 3, the resonance region is characterized by a pair of the positive and negative closed contours and moves to a smaller λ region as the value of $R\omega_E/v$ increases, and it comes near the boundary ($\lambda \cong 0$) provided $R\omega_E/v$ is larger than the critical value. Although the sudden changes of the transport coefficient mentioned above seems to come from the lack of the resolution in the region of $\lambda \cong 0$, this problem can be studied more clearly by the mesh accumulation to that region.

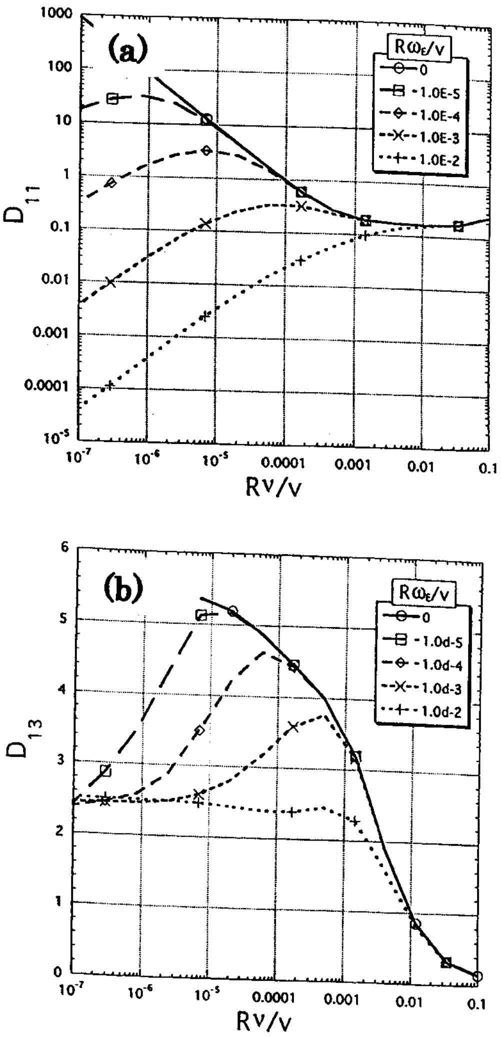

Fig. 1 Collisionality dependence of the diffusion coefficient (D_{11}),[1(a)] and the bootstrap current (D_{13}) [1(b)] for several values of the electric field.

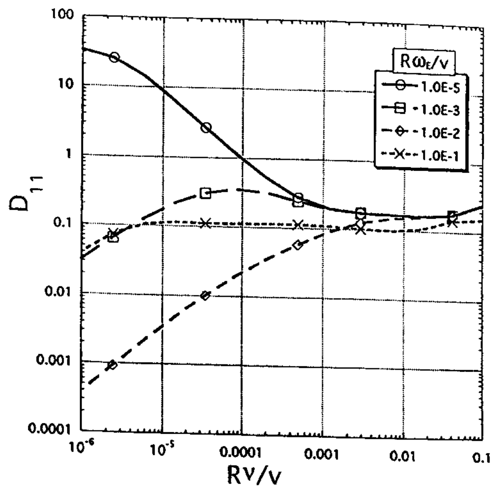

Fig. 2 Collisionality dependence of the diffusion coefficient (D_{11}) for several values of the electric field. Here, the case with $R\omega_E/v = 10^{-1}$ corresponds to the case of the resonance. Parameters used here are the same as Fig. 1.

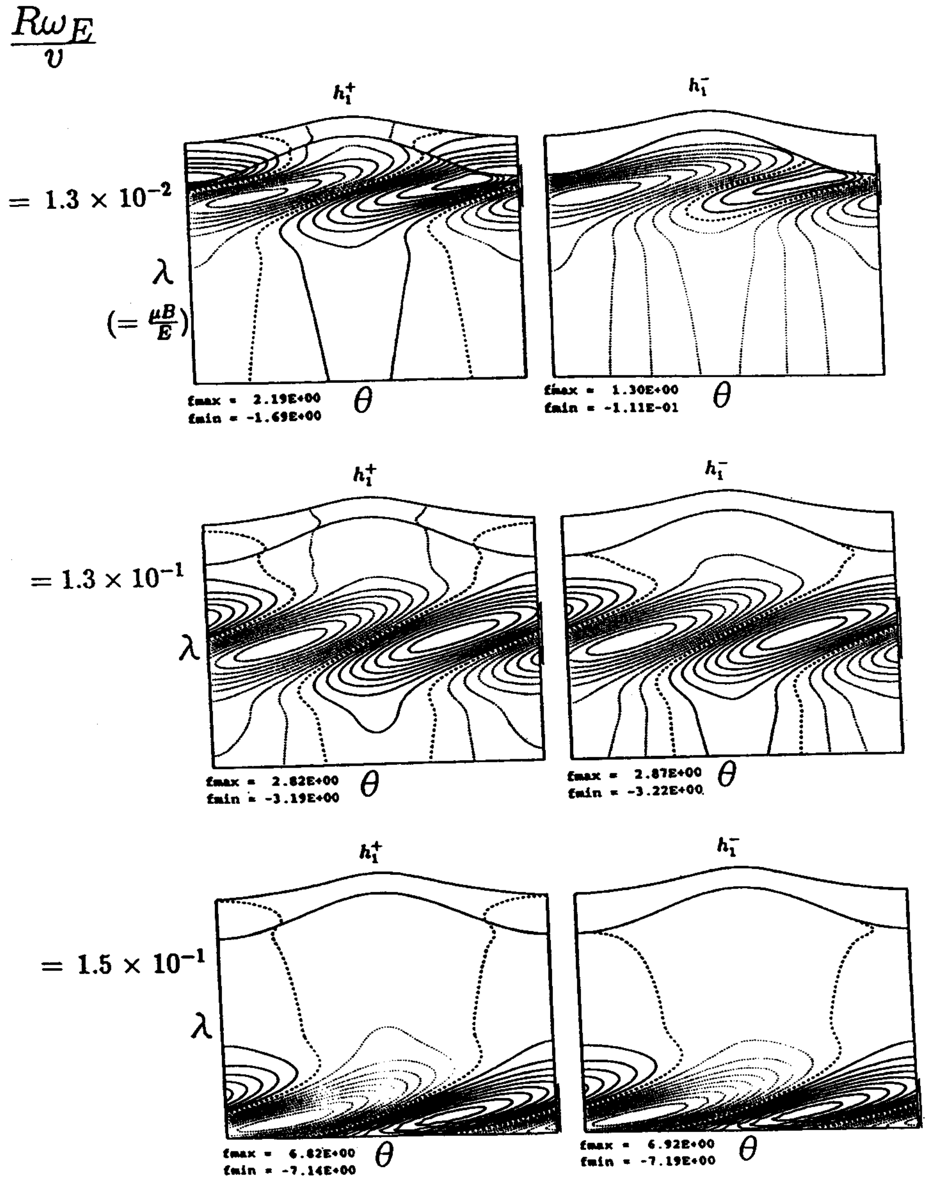

Fig. 3 Typical 2-D constant contours in the $\lambda - \vartheta$ plane for the even (h^+) and odd (h^-) parts of the distribution function are plotted for three typical values of the normalized electric field parameter.

4. Summary and Discussions

The numerical code solving the bounce averaged Fokker-Planck equation has been developed in the two dimensional space (λ, ϑ). The results obtained by the DKES code are reproduced by this code with less computation time. The 2-D contour plot of the distribution function revealed the importance of both the boundary layer effect and resonance effect on the results of the transports such as the bootstrap currents, as shown in Fig. 1(b). A better understanding of the influence of the electric field on the fine structure for the distribution function, the remarkable reduction of the diffusion coefficient, the degradation of the transport coefficient due to the resonance, and the novel behavior of the bootstrap current are obtained. However, more clear understandings of these phenomena await further investigations of the boundary layer contributions.

References

[1] S.P. Hirshman, K.C. Shaing, W.I. Van Rij, C.O. Beassley, Jr. and E.C. Crume, Jr., Phys. Fluids **29**, 2951 (1986).

[2] W.N.G. Hitchon, C.D. Beidler, H.E. Mynick and J.L. Shoet, Nucl. Fusion **25**, 105 (1985).

[3] J. Todoroki, J. Phys. Soc. Jpn. **59**, 2758 (1990).

[4] J. Todoroki and H. Sanuki, in *Proceedings of the International Conference on Plasma Physics* (ICPP96) in Nagoya (1996), pp.298–pp.301. See, also: H. Sanuki, J. Todoroki and T. Nakagawa, J. Accel. Plasma Res. **5**, No. 1 (2000) 53.

[5] H. Sanuki, J. Todoroki and T. Kamimura, Phys. Fluids B **2**, 2155 (1990).

[6] J. Todoroki, J. Phys. Soc. Jpn. **58**, 3979 (1989).

[7] Y. Ogawa, T. Amano, N. Nakajima, N. Ohyabu and K. Yamazaki, Nucl. Fusion **32**, 119 (1992).

[8] R. Kanno, N. Nakajima, H. Sugama, M. Okamoto and Y. Ogawa, Nucl. Fusion **37**, 1463 (1997).

[9] K.C. Shaing *et al.*, Phys. Fluids B **1**, 148 (1989).